Demonstrating Kondo behavior by temperature-dependent scanning tunneling spectroscopy

Elia Turco [1,*] Markus Aapro [2,†] Somesh C. Ganguli [2] Nils Krane [1]
Robert Drost,[2] Nahual Sobrino,[3] Annika Bernhardt,[4] Michal Juríček [4] Roman Fasel [1,5]
Pascal Ruffieux,[1] Peter Liljeroth [2] and David Jacob [3,6,‡]

[1]*nanotech@surfaces Laboratory, Empa - Swiss Federal Laboratories for Materials Science and Technology, 8600 Dübendorf, Switzerland*
[2]*Department of Applied Physics, Aalto University, 00076 Aalto, Finland*
[3]*Departamento de Polímeros y Materiales Avanzados: Física, Química y Tecnología, Universidad del País Vasco UPV/EHU, Av. Tolosa 72, E-20018 San Sebastián, Spain*
[4]*Department of Chemistry, University of Zurich, Winterthurerstrasse 190, 8057 Zurich, Switzerland*
[5]*Department of Chemistry, Biochemistry and Pharmaceutical Sciences, University of Bern, 3012 Bern, Switzerland*
[6]*IKERBASQUE, Basque Foundation for Science, Plaza Euskadi 5, E-48009 Bilbao, Spain*

The Kondo effect describes the scattering of conduction electrons by magnetic impurities, manifesting as an electronic resonance at the Fermi energy with a distinctive temperature evolution. In this Letter, we present a critical evaluation of the current methodology employed to demonstrate Kondo behavior in transport measurements, underscoring the limitations of established theoretical frameworks and the influence of extrinsic broadening. We introduce an approach for analyzing spectroscopic indicators of the Kondo effect, employing the Hurwitz-Fano lineshape as a model for the Kondo resonance in the presence of extrinsic broadening. Through precise scanning tunneling spectroscopy measurements on an exemplary spin-1/2 Kondo system, phenalenyl on Au(111), we demonstrate the efficacy of our proposed protocol in extracting accurate intrinsic Kondo linewidths from finite-temperature measurements. The extracted linewidths exhibit a robust fit with a recently derived expression for the temperature-dependent intrinsic Kondo linewidth, providing compelling evidence for the validity of the underlying theory.

The Kondo effect is one of the most enigmatic phenomena in condensed matter physics and one of the hallmarks of strong electronic correlations [1–4]. It occurs when a magnetic impurity interacts with the conduction electrons in a metallic host. Below a characteristic temperature, called the Kondo temperature, T_K, the impurity spin is effectively screened by the formation of a total spin-singlet state with the surrounding conduction electrons. As the low-temperature dynamics of individual Kondo impurities are governed by the energy scale $k_B T_K$, its magnitude has a major influence on the ground states and quantum phase diagrams of strongly correlated materials, such as Kondo lattices and heavy fermion systems [5–9].

The Kondo effect is signaled by the appearance of a sharp resonance at the Fermi level in the density of states of the magnetic impurity. This can be exploited for the detection of magnetic moments in atoms and molecules adsorbed on

metallic substrates by scanning tunneling spectroscopy (STS), where it shows up as a zero-bias anomaly in the conductance (dI/dV) spectra [10–14]. However, a clear-cut proof of Kondo behavior requires to discriminate the Kondo resonance from other zero-bias anomalies. This can be achieved, for example, by measuring the temperature evolution of the resonance's linewidth [15–19], which shows a characteristic universal behavior in the Kondo regime [20,21].

Attempts to derive an analytic expression for the temperature dependence of the Kondo peak from Fermi liquid theory [15] were shown to be problematic due to the limitation to very low temperatures $T \ll T_K$ and energies $\omega \ll \Gamma_K$ [22,23]. As a consequence, empirical expressions for the temperature-dependent Kondo linewidth are often used to fit experimental data, e.g., $\Gamma_{emp}(T) = \sqrt{(\alpha k_B T)^2 + 2(k_B T_{K,N})^2}$ where α was introduced as an additional fitting parameter instead of $\alpha = \pi$ as originally defined in Ref. [15]. Due to the free parameter α and different definitions for the Kondo temperature (e.g., $T_{K,N} = 2.77 \, T_K$) [24], various forms for $\Gamma_{emp}(T)$ can be found in the literature [16,17,19,25–27]. It has also been noted that simple square-root expressions such as $\Gamma_{emp}(T)$ cannot capture the universal scaling behavior obtained in accurate numerical renormalization group calculations [28].

Recently, an analytic equation for the temperature-dependent linewidth of the Kondo peak was derived from a novel theoretical Ansatz for the renormalized self-energy that

*elia.turco@empa.ch
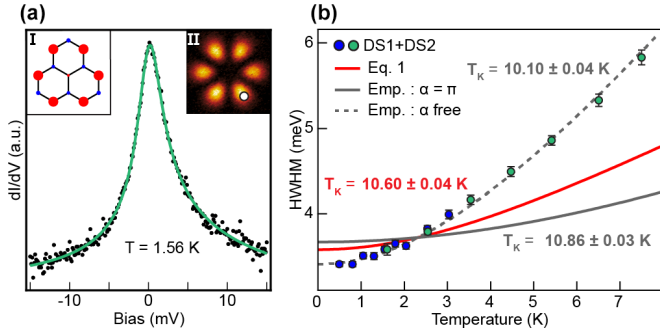†markus.aapro@aalto.fi
‡david.jacob@ehu.es

FIG. 1. (a) dI/dV spectrum of phenalenyl from DS2 at $T = 1.56$ K (black dots) showing the Kondo resonance, fitted by Frota-Fano lineshape (green line). Insets I and II show the theoretical and experimental spatial distribution of the unpaired electron [19]. (b) Kondo linewidths extracted from Frota fits to dI/dV spectra of DS1 (blue circles) and DS2 (green circles) versus temperature, and fits to Eq. (1) (red solid line), and to $\Gamma_{\mathrm{emp}}(T)$ with fixed $\alpha = \pi$ (gray solid line) and with α as fit parameter (gray dashed line, $\alpha = 7.45$). Error bars show the estimated standard deviation.

extends the temperature and energy range beyond the Fermi liquid regime [23]:

$$\Gamma(T) = \Delta_{\mathrm{K}} \cdot \sqrt{a + b\sqrt{1 + \left(\frac{\tau}{\Delta_{\mathrm{K}}}\right)^2} + c\left(\frac{\tau}{\Delta_{\mathrm{K}}}\right)^2}, \quad (1)$$

where $a \equiv 1 + \sqrt{3} \sim 2.732$, $b \equiv 2 + \sqrt{3} \sim 3.732$, and $c \equiv \sqrt{3}/2 \sim 0.866$ are constants, $\tau \equiv \pi k_{\mathrm{B}}T$ is the temperature parameter, and Δ_{K} the width parameter of the $T = 0$ Kondo peak, related to the halfwidth via $\Gamma_{\mathrm{K}} = 2.542\,\Delta_{\mathrm{K}}$ and to the Kondo temperature via $\Delta_{\mathrm{K}} = 1.542\,k_{\mathrm{B}}T_{\mathrm{K}}$ [29]. As shown in Ref. [23], Eq. (1) is in excellent agreement with numerical renormalization group calculations [21]. On the other hand, experimental data of Kondo linewidths versus temperature measured by STS [16] could not be fitted very well, most likely due to the presence of extrinsic broadening mechanisms in the STS data [30]. Post-hoc removal of extrinsic broadening from the experimentally measured widths only slightly improved the agreement. Therefore, a clear experimental proof of the theory of Ref. [23] is still lacking.

In this work, we demonstrate the validity of the theory reported in Ref. [23] by accurate temperature-dependent measurements and analysis of a prototypical spin-1/2 Kondo system, and provide an efficient protocol to experimentally prove the Kondo nature of a zero-bias peak. To this end, we carried out low-temperature STM experiments on phenalenyl molecules deposited on an Au(111) surface [24]. The unpaired π_z electron of phenalenyl forms an $S = 1/2$ ground state and is uniformly delocalized over six equivalent positions, as shown in the two insets of Fig. 1(a) where the spin density plot (inset I) and the experimental constant-height map of the Kondo resonance (inset II) are reported (more details in Ref. [19]). The high-resolution STS spectra shown in this work were measured with a metal STM tip and acquired as point spectra on one of the six equivalent Kondo lobes, as depicted in inset II of Fig. 1(a).

Two distinct data sets of temperature-dependent dI/dV spectra were acquired on two different molecules, which are

similarly adsorbed on the face centered cubic (*fcc*) region of the Au(111) herringbone reconstruction. We refer to the lower temperature data set as DS1, while DS2 is the data set from 1.56 K to 7.5 K. For each temperature the Kondo peak was fitted with the Frota-Fano lineshape [example shown in Fig. 1(a)], taking quantum interference into account via the Fano phase ϕ [31–33], $F(V) = F_0 \cdot \mathrm{Re}[e^{i\phi}/\sqrt{1 + iV/\Delta}]$ where F_0 is the amplitude, and Δ the Frota width parameter related to the halfwidth of the Frota-Fano lineshape by $\Gamma = \sqrt{3 + \sqrt{12}} \cdot \Delta = 2.542 \cdot \Delta$. The Frota-Fano lineshape yields good fits for all temperatures [24]. The obtained halfwidths of the Frota fits are shown in Fig. 1(b) for both data sets. The two data sets overlap neatly in the temperature range where both molecules have been measured, i.e., between 1.5 K and 3 K. This justifies the merging of both data sets in order to obtain a larger temperature range. Fitting Eq. (1) to the merged data set yields a relatively poor fit as shown by the red line in Fig. 1(b), although somewhat better than the empirical expression $\Gamma_{\mathrm{emp}}(T)$ with fixed temperature coefficient $\alpha = \pi$ (gray solid line), similar to the finding in Ref. [23].

We will now see that the mismatch with Eq. (1) is caused by extrinsic broadening mechanisms. In STS, the conductance spectra (dI/dV) are measured at finite temperatures T where the Kondo peak is broadened (i) due to the intrinsic temperature dependence of the Kondo peak [15,21,23], and (ii) due to the presence of different extrinsic broadening mechanisms in the STS measurement [30]. Thus, in order to obtain the actual intrinsic halfwidth Γ_{K} of the Kondo peak and demonstrate Kondo behavior, one has to first remove the extrinsic contributions from the measured HWHM. Assuming a noise-optimized (electronic and mechanical) experimental setup, the two main sources of extrinsic broadening are caused by Fermi-Dirac (FD) broadening of the tip and the voltage modulation for the lock-in detection. A good fit with $\Gamma_{\mathrm{emp}}(T)$ can only be obtained by using α as a free fitting parameter (dashed gray line).

In order to properly incorporate the most important broadening mechanisms into the analysis of the STS data we now resort to theory. The experimental situation of STS is depicted schematically in Fig. 2(a): A molecule (M) on a metallic substrate (S) is probed by an STM tip (T). Application of a voltage V to the sample drives a current I from the sample electrode via the molecule to the tip electrode. Typically, in STS the coupling of M to T is much weaker than the coupling of M to S. In this situation, also called ideal STM limit [34], M is effectively in equilibrium with S, and the dI/dV of the current from the tip to the molecule at the substrate is given by the convolution

$$G(V) \equiv \frac{dI}{dV} \propto \int d\omega\,[-f'(\omega)]\,A(\omega + eV), \quad (2)$$

where $f'(\omega) = -\beta/(4\cosh^2(\beta\omega/2))$ is the derivative of the tip's FD distribution, $\beta = 1/k_{\mathrm{B}}T$ with T the temperature at the tip, and $A(\omega)$ the spectral function of the molecule [35]. We assume a fully thermalized system so that tip and sample have the same temperature T.

The convolution of the spectral function $A(\omega)$ with the FD derivative $f'(\omega)$ leads to broadening of the Kondo resonance, to which we now simply refer to as FD broadening. This is
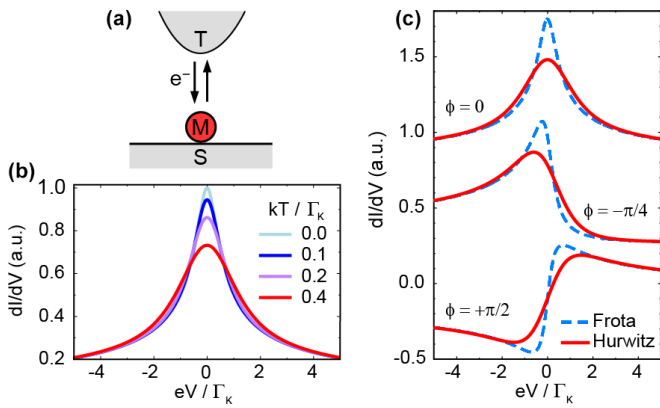
FIG. 2. (a) Schematic STM setup for measuring dI/dV spectra of a molecule (M) on a surface (S) by an STM tip (T). (b) Simulated dI/dV spectra assuming a Frota-Fano lineshape in the spectral function at different temperatures. (c) HF lineshapes (red solid lines) according to Eq. (3) at finite temperature $T = 0.4\,\Gamma_K/k_B$ and corresponding Frota-Fano lineshapes (blue dashed lines) in underlying spectral function for different values of ϕ and fixed halfwidth $\Gamma_K = 2.542\,\Delta_K$.
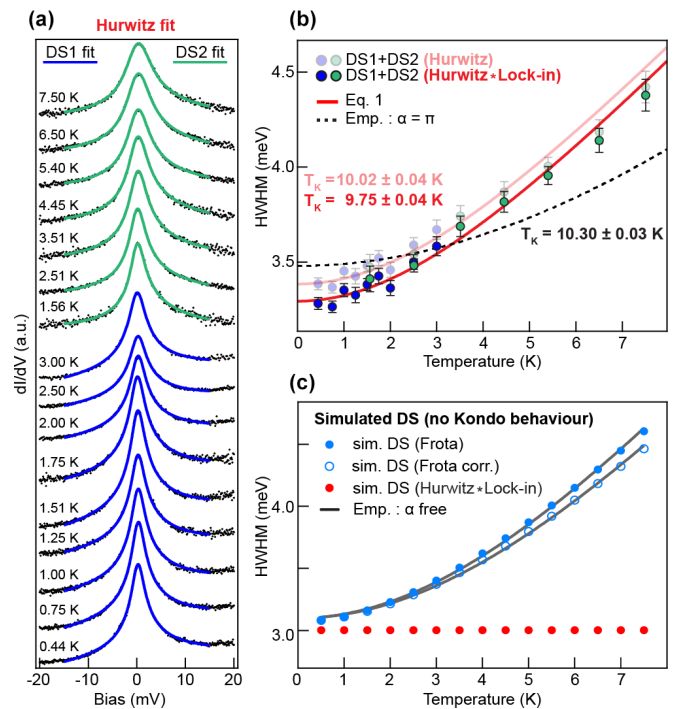

FIG. 3. (a) dI/dV spectra of DS1 and DS2 (black dots) fitted with HF lineshapes according to Eq. (3) (blue and green solid lines). (b) Intrinsic Kondo linewidths obtained from HF fits (transparent blue and green circles) versus temperature, fitted with Eq. (1) (transparent red line) and with $\Gamma_{emp}(T)$ with fixed $\alpha = \pi$ (black dashed line). Solid blue and green circles show intrinsic linewidths obtained from fitting with Eq. (4), taking into account both FD and lock-in broadening, fitted with Eq. (1) (solid red line). $V_m = 0.5$ mV for DS1 and $V_m = 0.4$ mV for DS2. Error bars show the estimated standard deviation. (c) Halfwidths versus temperature obtained from Frota (blue dots) and HF (red dots) fits for simulated data of Frota peak with constant intrinsic linewidth. Also shown are temperature corrected Frota widths (blue circles) using $\Gamma_{corr.}$ (see text). Gray lines show fits with $\Gamma_{emp}(T)$ resulting in $\alpha = 5.32$ (Frota) and $\alpha = 5.02$ (Frota corr.)

demonstrated in Fig. 2(b) which shows the numerically calculated dI/dV according to (2) for different tip temperatures, assuming a Frota-Fano peak for the spectral function, $A(\omega) \equiv F(\omega)$ with $\phi = 0$ and constant $\Delta = \Gamma_K/2.542$. Clearly, the effect is already considerable at temperatures of the order of $T_K \sim 0.25\,\Gamma_K/k_B$.

In order to obtain the intrinsic linewidth $\Gamma = 2.542\,\Delta$ of the Kondo resonance in the underlying spectral function, while taking into account a finite temperature T at the tip, we could simply fit (2) to the experimental dI/dV spectra. However, this requires to numerically evaluate the convolution (2) several times during the fitting procedure, leading to considerable computational effort, especially when lock-in modulation is also taken into account (see below). Instead, we now derive an analytic expression for the lineshape of the Kondo resonance in the dI/dV taking into account FD broadening, which allows to process the data very efficiently. A lineshape for the Kondo peak at finite temperature in the spectral function was recently given in Ref. [23]. This lineshape reduces to a Frota-Fano lineshape in the $T \rightarrow 0$ limit, but can also be well approximated by a Frota-Fano lineshape at finite T [21]. We therefore describe the Kondo resonance in the spectral function at some finite temperature T by the Frota-Fano lineshape, $A(\omega) \equiv F(\omega)$. The Frota width parameter Δ is determined by the intrinsic halfwidth of the Kondo peak Γ at temperature T according to (1), i.e., $\Delta = \Gamma(T)/2.542$. The resulting lineshape for the dI/dV can be expressed analytically in terms of the Hurwitz ζ function [24]:

$$G(V) \propto \sqrt{\frac{\Delta}{8\tau}} \cdot \mathrm{Re}\left[e^{i\phi} \zeta\left(\frac{3}{2}, \frac{\Delta}{2\tau} + \frac{1}{2} + i\frac{eV}{2\tau} \right) \right] \quad (3)$$

with the temperature parameter $\tau \equiv \pi k_B T$, as above. The Hurwitz ζ function is a generalization of the Riemann ζ function, and is defined by the infinite series $\zeta(s, a) = \sum_{n=0}^{\infty} 1/(n + a)^s$ where s and a can in general be complex, with $\mathrm{Re}[s] > 1$ and $n + a \neq 0$. Figure 2(c) shows these

Hurwitz-Fano (HF) lineshapes according to (3), as red solid lines corresponding to three different Frota-Fano lineshapes (shown as blue dashed lines) in the underlying spectral function $A(\omega)$ with different Fano phases ϕ as indicated in the plots.

The HF lineshape (3) can now be fitted [36] directly to the Kondo resonances in the finite-temperature dI/dV spectra recorded by STS, as shown in Fig. 3(a). We find that it fits the experimental data slightly better than the corresponding Frota fits [24]. Fitting the spectra with the HF lineshape yields smaller mean squared errors and the obtained width parameter Δ is also more consistent with varying the fit range [24]. Importantly, the Frota width parameter Δ resulting from each fit now yields the intrinsic halfwidth $\Gamma(T) = 2.542\Delta$ of the Kondo resonance for a given temperature T. As a result, the extracted halfwidths do follow the predicted intrinsic temperature broadening and can be fitted well by Eq. (1), as shown by the transparent red line in Fig. 3(b). This is in stark contrast to the halfwidths extracted from the corresponding Frota fits in Fig. 1(b).

Another important contribution to extrinsic broadening in STS experiments comes from the lock-in modulation of the bias voltage. The effect on the spectra can be described by a further convolution of the differential conductance $G(V)$ [27,30] as

$$\tilde{G}(V) = \int dV' \, \chi_m(V') \, G(V + V'), \qquad (4)$$

where the lock-in function χ_m is given by $\chi_m(V) = 2\sqrt{V_m^2 - V^2}/\pi V_m^2$ for $V \leqslant V_m$, and $\chi_m(V) = 0$ otherwise. $V_m = \sqrt{2}\,V_{rms}$ is the amplitude of the bias modulation. Thanks to the analytic solution (3) of the first convolution (2), this second convolution can be computed numerically efficiently enough to be used in the fitting procedure [36]. The resulting Frota width parameter Δ yields the Kondo width without the extrinsic broadening due to FD smearing or lock-in modulation. Thus, $\Gamma = 2.542\Delta$ now essentially yields the intrinsic halfwidth of the Kondo resonance at a given temperature T since the two most important STM inherent contributions of extrinsic broadening have been removed. Figure 3(b) shows in blue and green circles the intrinsic Kondo halfwidths extracted in this way, which can be fitted even better by Eq. (1), resulting in a mean square error of $MSE_{HL} = 1870\,\mu V^2$ compared to $MSE_H = 2474\,\mu V^2$ for the fits using just the HF lineshape. In order to visualize the effect of FD broadening in our experimental dataset (DS1 and DS2), in the Supplemental Material [24] we compare the linewidths from Fig. 1(b) (Frota fit) with the linewidths from Fig. 3(b) (Hurwitz fit), emphasizing the importance of removing extrinsic FD broadening.

So far we have shown the advantage of using the HF lineshape in order to directly obtain the intrinsic halfwidth of a Kondo resonance, as well as the validity of Eq. 1 to describe the correct temperature-dependent broadening of the intrinsic halfwidth. The combination of these two expressions is crucial for the verification of a Kondo resonance by its temperature dependence, as illustrated in Fig 3(c) for a simulated data set where a Frota lineshape of constant halfwidth ($\Gamma = 3$ mV) is broadened by FD and lock-in modulation ($V_m = 0.4$ mV). Fitting this data set with a Frota-Fano lineshape (blue dots) [24] yields an increasing halfwidth, whose temperature dependence can be fitted well with the empirical expression $\Gamma_{emp}(T)$, thus giving the false impression of Kondo behavior. Also the often employed temperature correction of the linewidth $\Gamma_{corr.} = \sqrt{\Gamma^2 - (1.75k_BT)^2}$ [16,19,25] does not properly compensate for the FD broadening, as shown by the blue circles in Fig 3(c). Using the HF lineshape, on the other hand, yields the correct constant linewidth of the underlying peak (red circles), revealing its non-Kondo nature. Similar results are obtained for a FD-broadened Lorentzian peak with a constant linewidth [24]. The empirical expression $\Gamma_{emp}(T)$ is therefore not a suitable proof for Kondo resonances and can only be used as an empirical way to extrapolate the Kondo temperature from such data sets if the presence of the Kondo effect can already be assumed.

On the other hand, if no proof of Kondo behavior is required, there is no need to perform temperature-dependent measurements in order to determine T_K. According to (1) the intrinsic halfwidth Γ at a certain temperature depends only on Δ_K and the (known) experimental temperature. The relation
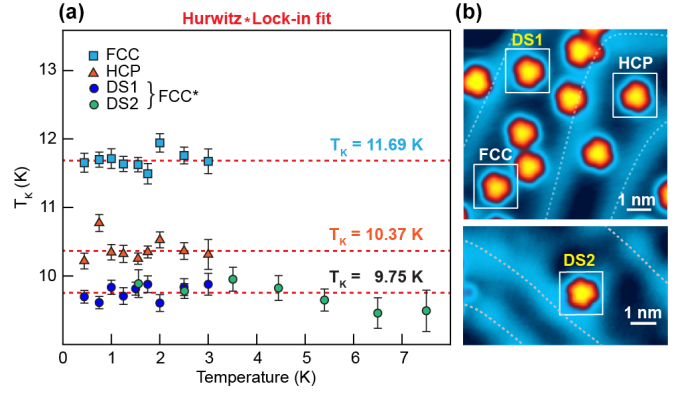

FIG. 4. (a) Kondo temperatures $T_K(T)$ determined for each dI/dV spectrum individually by HF $*$ Lock $-$ in fits [Eq. (4)] and using the resulting intrinsic linewidth Γ in Eq. (5). Error bars represent the estimated standard deviations. Red dashed lines indicate T_K obtained by fitting the temperature dependence of the Kondo linewidth for each adsorption site with Eq. (1) [24]. (b) STM images of phenalenyl molecules on Au(111) with boxes highlighting the investigated molecules. Scanning parameters for top image are $V = -2$ V, $I = 100$ pA and $V = -0.1$ V, $I = 50$ pA for the bottom image. Ridges of the herringbone reconstruction are marked with dashed white lines.

can therefore be rewritten as:

$$\Delta_K = \sqrt{\sqrt{\tfrac{1}{3}\Gamma^4 + \tfrac{1}{3}\tau^2\Gamma^2 + \alpha\tau^4} - \beta\tau^2 - \gamma\Gamma^2} \qquad (5)$$

where $\alpha \equiv (2 + \sqrt{3})/6 \sim 0.622$, $\beta \equiv 1 - 1/\sqrt{12} \sim 0.711$ and $\gamma \equiv 1 - 1/\sqrt{3} \sim 0.423$ are constants and $\tau \equiv \pi k_B T$ the temperature parameter. Using this relation, the Kondo temperature $T_K = \Delta_K/1.542k_B = \Gamma_K/3.92k_B$ [29] can be determined accurately from the intrinsic halfwidth of a single spectrum, taken at finite temperature. Figure 4(a) displays the T_K obtained from the individual spectra of data sets DS1 and DS2 in dark blue and green circles, respectively. There is less than 3% of variation between the individually determined Kondo temperatures and the T_K obtained before by fitting Eq. (1) to the linewidths as a function of temperature. Similarly consistent Kondo temperatures are found by applying this method to temperature-dependent data sets reported elsewhere [24]. The slight deviations from the expected constant behavior of the extracted T_K versus temperature may be attributed to experimental reasons, such as incomplete thermalization at higher temperatures [30].

We now apply the developed methodology to investigate the dependence of the Kondo temperature on the adsorption site of phenalenyl on the herringbone reconstruction of the Au(111) surface. Along with data sets DS1 and DS2, acquired on two molecules in the *fcc* region of the Au(111) reconstruction close to the herringbone ridge (adsorption site labeled as FCC*), we also carried out dI/dV measurements for phenalenyl adsorbed in the middle of the *fcc* (light blue) and *hcp* (orange) regions. By fitting each spectrum with a lock-in broadened HF lineshape and calculating T_K using (5), we find that different adsorption geometries result in different Kondo temperatures, as clearly shown in Fig. 4(a). This observation can be rationalized by slight changes in the hybridization between molecule and metal substrate and

the exponential dependence of the Kondo temperature on the hybridization [37]. The robustness of the single-point T_K determination, here shown for different adsorption sites and on an entire temperature series, justifies the use of this method as a fast and reliable route to estimate T_K of a Kondo system [38].

To conclude, we have performed accurate STS measurements of a pure spin-1/2 Kondo system, and developed tools for an efficient and accurate data analysis that properly takes into account extrinsic broadening of dI/dV spectra in STS. A key element of the methodology is an analytic expression for the Fermi-Dirac broadened Kondo lineshape in terms of the Hurwitz ζ function. Fitting the spectra with this Hurwitz-Fano lineshape yields the intrinsic width of the Kondo peak which fits very well with the recently derived expression (1) for the Kondo width as a function of temperature, proving the validity of the theory [23]. The procedure developed here allows to unequivocally prove Kondo behavior of a system probed by STS [36]. In contrast the established methodology of fitting the empirical expression $\Gamma_{emp}(T)$ to linewidths extracted from Frota fits to STS data may give a false impression of Kondo behavior. Finally, our methodology also allows to obtain the intrinsic Kondo width at $T = 0$ and corresponding Kondo temperature T_K from a single spectrum at finite temperature.

---

[1] J. Kondo, Resistance minimum in dilute magnetic alloys, Prog. Theor. Phys. **32**, 37 (1964).

[2] A. C. Hewson, *The Kondo Problem to Heavy Fermions* (Cambridge University Press, Cambridge, 1997).

[3] P. Fulde, *Electron Correlations in Molecules and Solids* (Springer, Berlin, 1995).

[4] P. Fazekas, *Lecture Notes on Electron Correlation and Magnetism* (World Scientific, Singapore-New Jersey-London-Hong Kong, 1999).

[5] P. Coleman, Heavy fermions: Electrons at the edge of magnetism, in *Handbook of Magnetism and Advanced Magnetic Materials* (John Wiley & Sons, Ltd., 2007).

[6] H. v. Löhneysen, A. Rosch, M. Vojta, and P. Wölfle, Fermi-liquid instabilities at magnetic quantum phase transitions, Rev. Mod. Phys. **79**, 1015 (2007).

[7] B. Keimer and J. E. Moore, The physics of quantum materials, Nat. Phys. **13**, 1045 (2017).

[8] W. Zhao, B. Shen, Z. Tao, Z. Han, K. Kang, K. Watanabe, T. Taniguchi, K. F. Mak, and J. Shan, Gate-tunable heavy fermions in a moiré Kondo lattice, Nature (London) **616**, 61 (2023).

[9] N. Roch, S. Florens, V. Bouchiat, W. Wernsdorfer, and F. Balestro, Quantum phase transition in a single-molecule quantum dot, Nature (London) **453**, 633 (2008).

[10] V. Madhavan, W. Chen, T. Jamneala, M. F. Crommie, and N. S. Wingreen, Tunneling into a single magnetic atom: Spectroscopic evidence of the Kondo resonance, Science **280**, 567 (1998).

[11] J. Li, W.-D. Schneider, R. Berndt, and B. Delley, Kondo scattering observed at a single magnetic impurity, Phys. Rev. Lett. **80**, 2893 (1998).

[12] H. C. Manoharan, C. P. Lutz, and D. M. Eigler, Quantum mirages formed by coherent projection of electronic structure, Nature (London) **403**, 512 (2000).

[13] O. Újsághy, J. Kroha, L. Szunyogh, and A. Zawadowski, Theory of the fano resonance in the STM tunneling density of states due to a single Kondo impurity, Phys. Rev. Lett. **85**, 2557 (2000).

[14] A. Schiller and S. Hershfield, Theory of scanning tunneling spectroscopy of a magnetic adatom on a metallic surface, Phys. Rev. B **61**, 9036 (2000).

[15] K. Nagaoka, T. Jamneala, M. Grobis, and M. F. Crommie, Temperature dependence of a single Kondo impurity, Phys. Rev. Lett. **88**, 077205 (2002).

[16] S. Mishra, D. Beyer, K. Eimre, S. Kezilebieke, R. Berger, O. Gröning, C. A. Pignedoli, K. Müllen, P. Liljeroth, P. Ruffieux, X. Feng, and R. Fasel, Topological frustration induces unconventional magnetism in a nanographene, Nat. Nanotechnol. **15**, 22 (2020).

[17] J. Li, S. Sanz, J. Castro-Esteban, M. Vilas-Varela, N. Friedrich, T. Frederiksen, D. Peña, and J. I. Pascual, Uncovering the triplet ground state of triangular graphene nanoflakes engineered with atomic precision on a metal surface, Phys. Rev. Lett. **124**, 177201 (2020).

[18] S. Mishra, G. Catarina, F. Wu, R. Ortiz, D. Jacob, K. Eimre, J. Ma, C. A. Pignedoli, X. Feng, P. Ruffieux, J. Fernández-Rossier, and R. Fasel, Observation of fractional edge excitations in nanographene spin chains, Nature (London) **598**, 287 (2021).

[19] E. Turco, A. Bernhardt, N. Krane, L. Valenta, R. Fasel, M. Jurek, and P. Ruffieux, Observation of the magnetic ground state of the two smallest triangular nanographenes, JACS Au **3**, 1358 (2023).

[20] T. A. Costi, Kondo effect in a magnetic field and the magnetoresistivity of Kondo alloys, Phys. Rev. Lett. **85**, 1504 (2000).

[21] Ž. Osolin and R. Žitko, Padé approximant approach for obtaining finite-temperature spectral functions of quantum impurity

models using the numerical renormalization group technique, Phys. Rev. B **87**, 245135 (2013).

[22] C. Chen, I. Sodemann, and P. A. Lee, Competition of spinon Fermi surface and heavy Fermi liquid states from the periodic Anderson to the Hubbard model, Phys. Rev. B **103**, 085128 (2021).

[23] D. Jacob, Temperature evolution of the Kondo peak beyond Fermi liquid theory, Phys. Rev. B **108**, L161109 (2023).

[24] See Supplemental Material at http://link.aps.org/supplemental/10.1103/PhysRevResearch.6.L022061 for method details, complementary experimental results and simulations.

[25] Y.-h. Zhang, S. Kahle, T. Herden, C. Stroh, M. Mayor, U. Schlickum, M. Ternes, P. Wahl, and K. Kern, Temperature and magnetic field dependence of a Kondo system in the weak coupling regime, Nat. Commun. **4**, 2110 (2013).

[26] A. A. Khajetoorians, M. Valentyuk, M. Steinbrecher, T. Schlenk, A. Shick, J. Kolorenc, A. I. Lichtenstein, T. O. Wehling, R. Wiesendanger, and J. Wiebe, Tuning emergent magnetism in a Hund's impurity, Nat. Nanotechnol. **10**, 958 (2015).

[27] T. Esat, T. Deilmann, B. Lechtenberg, C. Wagner, P. Krüger, R. Temirov, F. B. Anders, M. Rohlfing, and F. S. Tautz, Transferring spin into an extended π orbital of a large molecule, Phys. Rev. B **91**, 144415 (2015).

[28] See Supplemental Note 12 of Ref. [39].

[29] Here as in Ref. [23] we use Wilson's thermodynamic definition of T_K [40], corrected by Wiegman and Tsvelick [41]. As shown in Ref. [23] T_K is related to the halfwidth Γ_K of the Kondo peak by $T_K \sim \Gamma_K/3.92$.

[30] M. Gruber, A. Weismann, and R. Berndt, The Kondo resonance line shape in scanning tunnelling spectroscopy: Instrumental aspects, J. Phys.: Condens. Matter **30**, 424001 (2018).

[31] H. O. Frota, Shape of the Kondo resonance, Phys. Rev. B **45**, 1096 (1992).

[32] H. Prüser, M. Wenderoth, A. Weismann, and R. G. Ulbrich, Mapping itinerant electrons around Kondo impurities, Phys. Rev. Lett. **108**, 166604 (2012).

[33] S. Frank and D. Jacob, Orbital signatures of Fano-Kondo lineshapes in STM adatom spectroscopy, Phys. Rev. B **92**, 235127 (2015).

[34] D. Jacob and S. Kurth, Many-body spectral functions from steady state density functional theory, Nano Lett. **18**, 2086 (2018).

[35] For noninteracting electrons, Eq. (2) can be derived from Bardeen tunneling theory, see, e.g., Ch. 21.8 in Ref. [42]. For interacting electrons it can be derived from the Meir-Wingreen equation [43] assuming the ideal STM limit, see Ref. [34].

[36] Python and Igor programs for fitting Hurwitz and Hurwitz $*$ Lock $-$ in lineshapes are publically available on GitHub at https://github.com/david-jacob/HurwitzFanoFit.

[37] F. D. M. Haldane, Theory of the atomic limit of the Anderson model: I. Perturbation expansions re-examined, J. Phys. C: Solid State Phys. **11**, 5015 (1978).

[38] An alternative route for determining T_K from STS at $T \sim T_K$, recently proposed in Ref. [44], requires additional control parameters in the experiment such as magnetic field or mechanical gating.

[39] C. van Efferen, J. Fischer, T. A. Costi, A. Rosch, T. Michely, and W. Jolie, Modulated Kondo screening along magnetic mirror twin boundaries in monolayer MoS_2, Nat. Phys. **20**, 82 (2024).

[40] K. G. Wilson, The renormalization group: Critical phenomena and the Kondo problem, Rev. Mod. Phys. **47**, 773 (1975).

[41] P. B. Wiegmann and A. M. Tsvelick, Exact solution of the Anderson model: I, J. Phys. C **16**, 2281 (1983).

[42] B. Voigtländer, *Scanning Probe Microscopy* (Springer, Berlin Heidelberg, 2015).

[43] Y. Meir and N. S. Wingreen, Landauer formula for the current through an interacting electron region, Phys. Rev. Lett. **68**, 2512 (1992).

[44] M. Žonda, O. Stetsovych, R. Korytár, M. Ternes, R. Temirov, A. Raccanelli, F. S. Tautz, P. Jelínek, T. Novotný, and M. Švec, Resolving ambiguity of the Kondo temperature determination in mechanically tunable single-molecule Kondo systems, J. Phys. Chem. Lett. **12**, 6320 (2021).